E-143

SLAC Proposal
End Station A

Measurement of the Nuclear Dependence and Momentum Transfer Dependence of Quasielastic (e,e'p) Scattering at Large Momentum Transfer

&

Measurement of Nuclear Structure Functions at $x > 1$ and Large Momentum Transfer

American University
Argonne National Laboratory
California Institute of Technology
California State University, Los Angeles
Rensselaer Polytechnic Institute
Lawrence Livermore National Laboratory
Massachusetts Institute of Technology
Stanford Linear Accelerator Center
University of Basel
University of Colorado
University of Illinois
University of Virginia
University of Wisconsin-Madison

May 1992

ABSTRACT

We present two experiments, color transparency and nuclear structure functions at $x > 1$, that use a new 16 GeV/c spectrometer and the present 8 GeV/c spectrometer. These experiments require the full Linac beam to End Station A, and use virtually the same detector packages, electronics, and data acquisition.

We propose to make coincidence measurements of the quasielastic (e,e'p) cross section on several nuclei in the Q^2 range of 6 to 15 $(\mathrm{GeV/c})^2$ using the 23 GeV linac beam and spectrometers in End Station A at SLAC. A fixed-angle magnetic spectrometer will be constructed from existing SLAC magnets and used for detection of quasielastically scattered electrons. The presently configured 8 GeV/c spectrometer will be used for detection of recoil protons with momenta up to 8.9 GeV/c. Because of the kinematic focussing of the recoil protons which occurs at high Q^2, a large fraction of the Fermi cone is accepted in the kinematic range of the experiment. The measurement will have sufficient missing energy resolution to determine that the struck proton did not emit a pion. The proposed measurements will significantly extend those recently carried out by members of this collaboration in experiment NE18. Beam energies from 12.1 to 23 GeV at maximum current will be required from the SLAC linac. The goal of the experiment is to study quasielastic scattering from nuclei at high Q^2 as an exclusive process in QCD, and in particular to look for evidence of color transparency. All theoretical calculations that include color transparency predict large effects in the kinematic region of the proposed experiment.

We also propose an inclusive electron-nucleus scattering experiment in the domain of large x and Q^2, to measure the nuclear structure function F_2^A. Previous data for $x > 1$ have been limited to $Q^2 < 4$ $(\mathrm{GeV/c})^2$. We propose to extend this Q^2 range for $x = 2$ up to $Q^2 = 7$ $(\mathrm{GeV/c})^2$ and $x = 1.2$ up to $Q^2 = 40$ $(\mathrm{GeV/c})^2$. These data can provide important information on the scaling of the nuclear structure function, constrain the components of the nuclear wave function at large momentum and binding energy, and put limits on non-nucleonic degrees of freedom in nuclei. In addition, these inclusive data may also provide complementary information on color transparency.

These two experiments address complementary physics issues and make use of the same apparatus. They require the assembly of a new fixed-angle 16 GeV/c spectrometer and a fully instrumented 8 GeV/c spectrometer. The detector packages can be assembled from existing hardware in End Station A. The beam requirements are one beam month or two calendar months at 50% efficiency of long-pulse running at energies from 8 - 23.5 GeV.

I. Color Transparency

1.1 Introduction

Measurement of exclusive processes from nuclei at high Q^2 is important as a constraint on the theory of the strong interaction [I.1]. Where perturbative QCD (PQCD) is applicable, the scattering process can be understood in terms of a simple counting rule argument [I.2] and indeed the Q^2 dependence of the prediction is in agreement with the measured cross section for many exclusive processes at high momentum transfer [I.3]. However, significant problems arise when one undertakes a more detailed calculation [I.4] and the question of the applicability of PQCD in exclusive processes remains an open question. The argument centers on how much of the interaction is described by processes which are hard (strong interactions acting for a short time and over a distance small compared to ~ 1 fermi) and how much by processes which are soft (strong interactions acting over distance scales of order 1 fermi).

The high Q^2 measurement of quasielastic (e,e'p) scattering from nuclei by the recently completed SLAC experiment NE18 has increased the maximum momentum transfer by about one order of magnitude to 6.8 $(\mathrm{GeV/c})^2$. In this proposal we propose to extend the measurements up to $Q^2 = 15(\mathrm{GeV/c})^2$. The motivation is a striking prediction of PQCD for the (e,e'p) quasielastic process in nuclei. At large momentum transfer, diminishing elastic and inelastic final-state interactions of the recoil proton in the nuclear medium are predicted [I.5,6]. This effect is called "color transparency". These measurements can provide important information on the applicability of PQCD to exclusive processes.

Measurements have been carried out in quasielastic (p,2p) scattering at Brookhaven and an energy dependence to the transparency has been observed [I.7]. This has been interpreted as evidence for soft contributions due to high mass dibaryon resonances [I.8] or Landshoff contributions [I.9]. However, the (p,2p) data contain little information on the missing energy distribution of the struck nucleon. In addition, the p-p elastic scattering cross section contains an oscillation superimposed on the hard scattering scaling behaviour. Further (p,2p) measurements are underway [I.10] in a Q^2 regime comparable to that in the measurements proposed here.

Quasielastic proton knockout with an electron probe is intrinsically cleaner because of the known electromagnetic interaction and the absence of oscillations in the basic elastic cross section. It is the purpose of the experiment outlined in this proposal to extend measurements of the (e,e'p) coincidence quasielastic cross section in nuclei out to $Q^2 = 15$ $(\mathrm{GeV/c})^2$, attainable with the full energy of the SLAC linac. The common result in

all calculations of color transparency phenomena is an increase in transparency effects with increasing Q^2. In the region of NE18 kinematics, i.e. $Q^2 \leq 7$ $(GeV/c)^2$, the color transparency effects may be expected to first turn on. Analysis of the NE18 data will set a strong constraint on effects for $Q^2 \leq 7$ $(GeV/c)^2$. However, many theoretical calculations predict a large enhancement in the kinematic region up to $Q^2 = 15$ $(GeV/c)^2$. The SLAC linac and End Station A equipment represent the world's only facility with the combination of high energy and high luminosity necessary to carry out this important experiment.

1.2 Physics Motivation

QCD has the important simplifying feature at high Q^2 of asymptotic freedom [I.11]. This implies that the magnitude of the strong coupling constant should diminish as Q^2 increases. This permits the use of perturbation theory in QCD calculations. This theory has been quite successful in the areas of deep inelastic scattering of leptons from nucleons [I.12], hadron-hadron collisions at large transverse momentum [I.13], baryon and meson spectroscopy [I.14], and jets in e^+e^- and hadronic collisions [I.15].

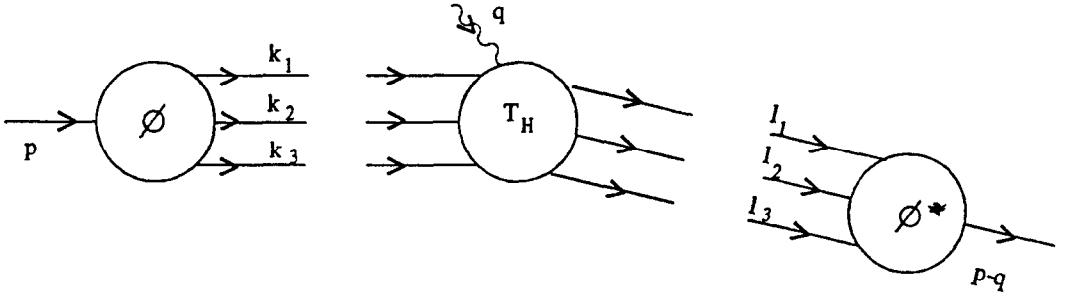

Figure I.1. Factorization of the scattering amplitude for exclusive processes involving nucleons. The distribution amplitudes Φ contain the nonperturbative dynamics of the nucleon. The hard scattering kernel T_H is calculated in perturbation theory.

Exclusive processes such as elastic electron-proton scattering have been recognized as an important area of interest from the point of view of QCD. The basic calculational technique [I.3] is to separate the process into an interaction term, which is calculated perturbatively, and distribution amplitudes or wavefunctions which describe the non-perturbative amplitude for finding the hadrons to be in any given state. This is shown schematically in Fig. I.1. The interaction kernel describes the hard scattering amplitude, contains the main

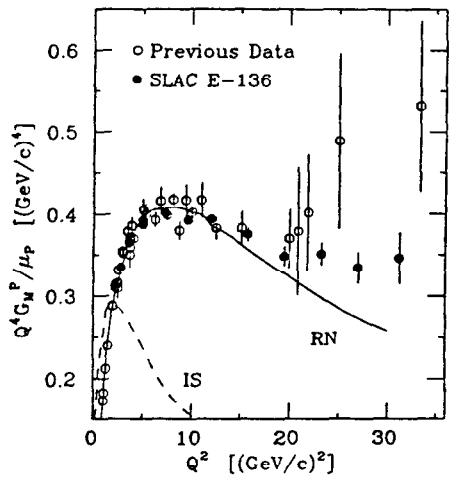

Figure I.2. Extracted values of $Q^4 G_M^p/\mu_P$ vs. Q^2 for elastic scattering on the proton.

dynamical dependence of the perturbative calculation, and can be calculated in terms of quark-gluon subprocesses.

The most striking consequence of QCD predictions for exclusive processes at large momentum transfer is the power-law behaviour of the form-factors. Brodsky and Farrar showed [I.3] that in any scale-invariant theory, of which QCD is an example, the power-law fall-off of helicity conserving form-factors is

$$F_H = \frac{1}{(Q^2)^{n_H - 1}}$$

where n_H is the number of constituent fields in H. In particular, for the proton we expect $G_M^p \sim Q^{-4}$ at high Q^2. In this regime the perturbative methods described above should be applicable. The data [I.16] are shown in Fig. I.2. We see that for $Q^2 \geq 5(\mathrm{GeV/c})^2$ the data begin to display the power-law behaviour. Since color transparency is directly related to hard scattering, this kinematic regime is very interesting for studying effects predicted by perturbative QCD. Note that this is somewhat controversial since the origin of this smooth behavior of the form factor may also be the result of an accidental conspiracy of soft processes mimicking the perturbative prediction [I.4].

At large Q^2 in elastic electron-proton scattering the virtual photon probes the small spatial components of the proton wave-function, since at large Q^2 the scattering occurs through the exchange of large transverse momenta between the quarks. As a consequence of the uncertainty principle, the transverse spatial extent of the struck proton is of order $\frac{1}{Q}$. Thus, in high Q^2 electron-proton elastic scattering the recoil proton must have a diminished

diminished transverse size. If we consider elastic electron-proton scattering as a quasielastic process inside a nucleus, the recoiling proton at high Q^2 will have a smaller transverse size than a normal proton and so will have a smaller interaction with the surrounding nucleons. This can be understood in a simple color Van-der-Waals model for the strong interaction where a smaller size implies a smaller color dipole moment, and a smaller interaction strength. This novel effect, predicted independently by Mueller [I.5] and Brodsky [I.6], is called "color transparency".

Farrar, Liu, Frankfurt, and Strikman (FLFS) [I.17] have quantitatively investigated whether one can expect to observe the nuclear transparency effect in quasielastic scattering from nuclei. They use a model based on the above physical assumptions to study the dynamics of transverse shrinkage. FLFS have calculated the onset of nuclear transparency for two particular models of the evolution - (1) the naive parton model, and (2) a PQCD model they term quantum diffusion. The results of their calculation are shown in Fig. I.3.

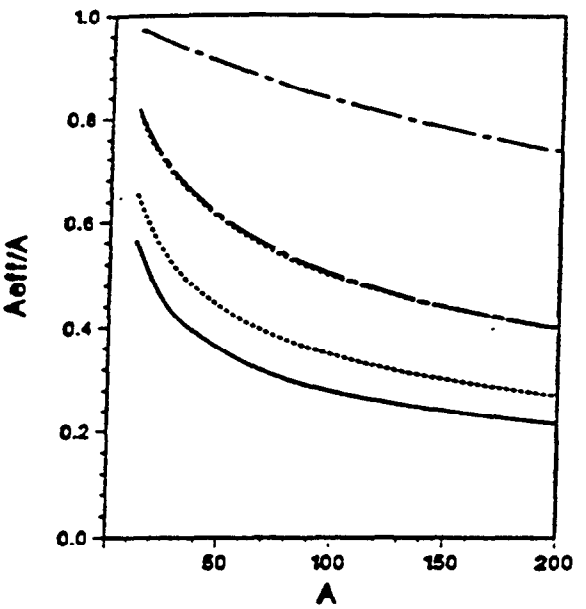

Figure I.3. The nuclear transparency as estimated by the calculation of FLFS [I.17] for quasielastic electron scattering on nuclei as a function of A and Q^2. $\tau = 0$ is the solid line; the dotted line is the model $\tau = 1$ and the dot-dashed line is the model $\tau = 2$. The transparency is calculated for each of these models at $Q^2 = 5$ $(GeV/c)^2$ (smaller transparency) and $Q^2 = 20$ $(GeV/c)^2$ (larger transparency).

Ralston and Pire [I.9] have carried out a quantum description of color transparency (QCT) in terms of light-cone operator matrix elements. For quasielastic electron knockout

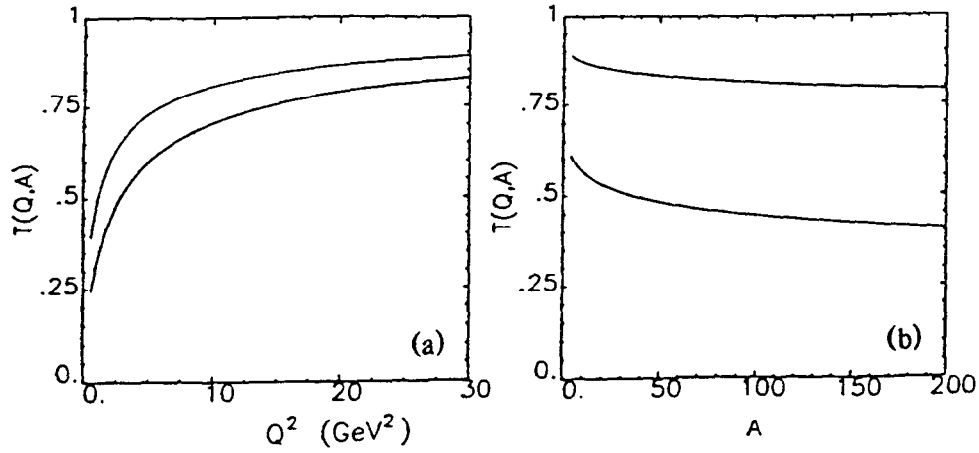

Figure I.4. Model QCT factor $T(Q, A)$ [I.9] relating the nuclear light-cone distribution amplitude to the free-space one. (a) At fixed A, the transparency amplitude increases with increasing Q^2; A = 12(200) for the upper (lower) curve. (b) At fixed Q^2, the transparency amplitude decreases with increasing A; Q^2 = 2(20) $(GeV/c)^2$ for the lower (upper) curve.

they predict a transparency amplitude $T(Q, A)$ which is shown in Fig. I.4.

Jennings and Miller [I.18] model the interaction between the quarks in the fast recoiling proton using soft (dipole) gluon exchange. They calculate the recoil-nucleon effective cross section by using a hadronic basis and the eikonal approximation. Fig. I.5 shows their calculation for ^{56}Fe(e,e'p) as a function of the momentum transfer of the struck nucleon.

We see that the common result in the calculations is an increase in transparency effects with increasing Q^2. In the region of NE18 kinematics, i.e. $Q^2 \leq 7$ $(GeV/c)^2$, the calculations indicate the initial onset of color transparency effects. However, most theoretical calculations predict **large** enhancements in the kinematic region of the proposed measurements. Data on quasielastic (e,e'p) scattering from nuclei at these high momentum transfers will provide important information on the question of the applicability of PQCD to exclusive processes.

1.3 Experimental Overview

Recently, this collaboration (NE18) successfully carried out measurements of quasielastic (e,e'p) scattering from nuclei in the region $1 \leq Q^2 \leq 7$ $(GeV/c)^2$ on deuterium, carbon, iron, and gold targets. Analysis of this data is in progress and results are antici-

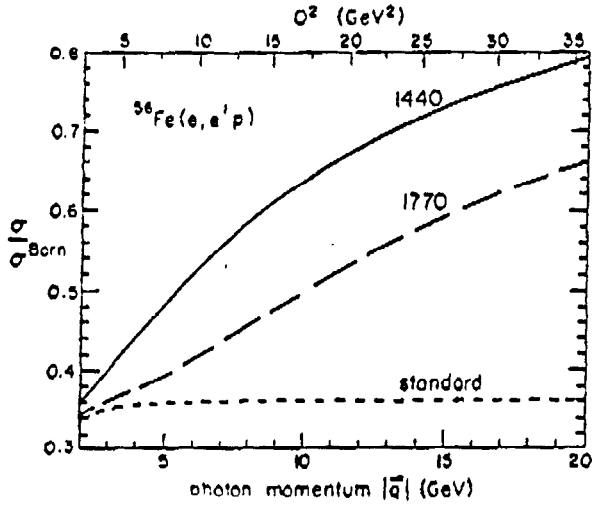

Figure I.5. The (e,e'p) reaction for a ^{56}Fe target [I.18]. The numerators are calculated using color transparency with different characteristic masses in the quantum expansion (solid = 1440 MeV, dashed = 1770 MeV) or the Glauber calculation (standard). The denominator is the Born approximation.

pated within 6 months. NE18 employed the Nuclear Physics Injector (E = 2 to 5.2 GeV) in conjunction with the 1.6 GeV/c electron spectrometer and the 8 GeV/c spectrometer for recoil proton detection. The spectrometers were configured for optimal double-arm timing resolution which was crucial for accidental background rejection. Further, a complete off-line data analysis package was written to analyze the data once the coincidence events were written to disk. NE18 demonstrated that the $\sim 2 \times 10^{-4}$ duty factor of the SLAC linac is adequate for high Q^2 quasielastic (e,e'p) measurements. Fig. I.6 shows the corrected coincidence timing peak from the carbon target at $Q^2 = 1$ (GeV/c)^2 with a FWHM of better than 600 ps.

The lowest count rate in NE18 was with the gold target at the highest Q^2. Fig. I.7 demonstrates the ability to measure the ^{197}Au(e,e'p) cross section at $Q^2 = 7$ (GeV/c)^2 where off-line analysis clearly resolves a coincidence peak with a coincidence counting rate of 2 counts/hour.

We propose to use a fixed-angle 16 GeV/c spectrometer and the present 8 GeV/c spectrometer in the large solid angle optics mode to detect quasielastically scattered electrons and recoil protons respectively. In this configuration we will be able to perform (e,e'p) coincidence experiments up to a momentum transfer of $Q^2 = 15$ (GeV/c)^2, significantly higher than the previous NE18 experiment.

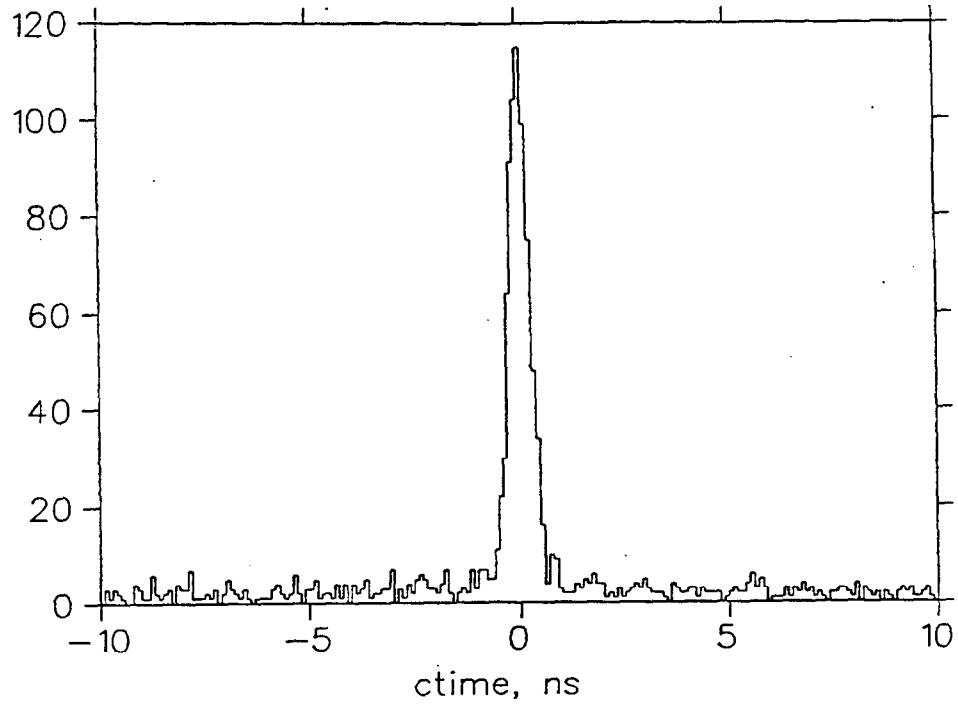

Figure I.6. Coincidence timing peak for ^{12}C at $Q^2 = 1$ (GeV/c)^2.

The fixed-angle 16 GeV/c spectrometer will be built on the floor of End Station A and set at a fixed forward angle of 13.5° to optimize coincidence count rates. This spectrometer will be configured from magnets of the existing 20 GeV/c spectrometer. The first and second order matrix elements for the 16 GeV/c system were calculated using the code TURTLE, and used in a Monte Carlo program to calculate the solid angle (see Section III).

The kinematic range explored in an (e,e'p) experiment is usually characterized by the missing momentum $\mathbf{p_m}$ and missing energy E_m. These are given by

$$\mathbf{p_m} = \mathbf{q} - \mathbf{p'},$$

$$E_m = \nu - T' - \frac{\mathbf{p_m}}{2M_{A-1}},$$

where $(\mathbf{q}, \nu)$ is the four-vector of the virtual photon and $(\mathbf{p'}, T' + M_p)$ is the four-vector of the knocked-out proton. The last term in the E_m definition accounts for the kinetic energy of the residual A-1 system. The missing energy resolution at high energies in quasielastic (e,e'p) scattering measurements at SLAC is dominated by the contribution from the incident beam energy. Table I.1 shows the missing energy resolution for the four proposed Q^2. We have assumed ±0.15% energy slits for the $Q^2 = 6$ (GeV/c)^2 point and

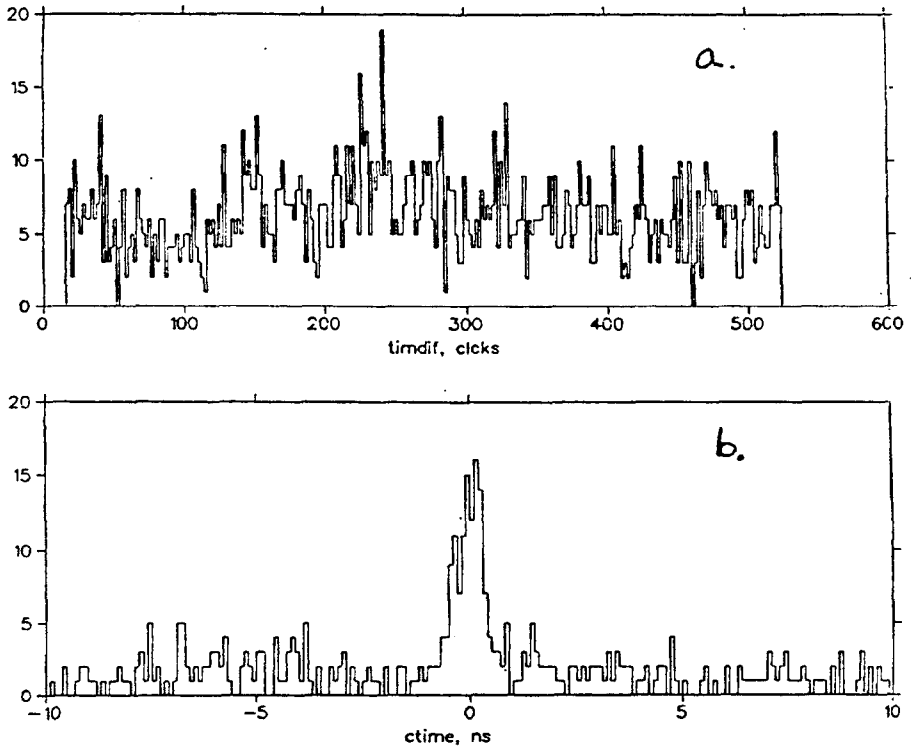

Figure I.7. (a) Uncorrected and (b) corrected coincidence timing peak for ^{197}Au(e,e'p) at $Q^2 = 7$ (GeV/c)^2.

$\pm 0.1\%$ energy slits for the $Q^2 = 9$, 12, and 15 (GeV/c)^2 points. In addition, we have assumed an electron arm momentum resolution of 0.15 %, and a proton arm momentum resolution of 0.15%. The contribution due to energy straggling in the target is negligible (a few MeV). The missing energy resolution is dominated by the contribution from the incident beam energy. The energy slits are chosen such that the resulting energy resolution is smaller than about 45 MeV. This is considered to be adequate for this experiment.

1.4 Run Plan

We will take data at four different Q^2 and so will require four different incident beam energies. Table I.2 presents an overview of the kinematics. Singles rates and ratio of accidental to true events for the proposed experiment are included for a 9% iron target.

The calculated run times assume 6% r.l. thick carbon target, a 9% iron target, 12% gold target, and liquid hydrogen and deuterium targets of 1.6% r.l. thick. 120 pulses per second with 5×10^{11} electrons per pulse is assumed for the beam current. The solid angle for the 8 GeV/c spectrometer is calculated for each kinematics separately, since it is determined by the maximum amount of focussing possible with the first two quadrupoles in the large acceptance optics mode. The acceptance of the 16 GeV/c spectrometer is discussed

Table I.1. Missing Energy Resolution (Full Width)

Q^2	E	E'	P	δ_E	$\delta_{E'}$	δ_p	$\sqrt{\delta_E^2+\delta_{E'}^2+\delta_p^2}$
$(GeV)^2$	GeV	GeV	GeV	MeV	MeV	MeV	MeV
15.0	21.0	13.0	8.9	42.0	19.5	13.3	48.0
12.0	18.3	11.9	7.3	36.6	17.9	11.0	42.0
9.0	15.4	10.6	5.7	30.8	15.9	8.6	36.0
6.0	12.1	8.9	4.0	36.3	13.4	6.0	39.0

in Section III. The coincidence rate has been determined by scaling the experimental coincidence rates as found in the NE18 experiment. This scaling involves calculating the electron-proton cross section times a kinematical factor reflecting the three-body reaction A(e,e'p)B and then by calculating the fraction of the quasielastically knocked-out protons that are scattered into the 8 GeV/c spectrometer. In determining the losses due to final state interactions we have assumed no transverse shrinkage and used the conventional Glauber calculation of Fig. I.5. We remark that if the FLFS [I.17] calculation is correct, we will see a large enhancement over our calculated coincidence rate in heavier nuclei at these high Q^2. The electron singles rate is determined by adding both the inclusive quasielastic contribution and the Fermi-smeared deep-inelastic contribution. The hadron singles rate is determined from parameterization of previous measurements with incident bremsstrahlung photons of energy 5-19 GeV. This parameterization gave good agreement with the measured hadron singles rates in NE18.

At each Q^2 we shall carry out measurements of the A(e,e'p) cross section over a missing energy range of 0 to 140 MeV and a recoil momentum range of 0 to 250 MeV/c. Only one kinematical setting is required, with the incident energy and $p' \approx q$ kept fixed. The experiment requires one calendar month of long-pulse running, assuming a total efficiency of 50%.

Table I.2. Kinematics and rates for the proposed experiment assuming an average beam current of 10 μA. The counting rates assume no transverse shrinkage of the final proton, corresponding to the lowest experimental rate. A resolving time of 1.0 ns and a duty factor of 2×10^{-4} are assumed in the calculation of the ratio of accidentals to trues. The total times for each target are: D: 45 hrs, C: 180 hrs, Fe: 360 hrs, Au: 200 hrs, e-p elastic calibration and empty target: 35 hrs.

Q^2	E	E'	P_s	θ_p	Target	R_c	R_e	R_p	A/T	#counts
$(GeV/c)^2$	GeV	GeV	GeV/c			(/hr)	(Hz)	(Hz)		
6.0	12.1	8.9	4.0	31.3	LH2_15cm	9000	2.7		0	5000
					LD2_15cm	1700				1000
					C_6%	240				500
					FE_9%	73	11.4	103	.40	400
9.0	15.4	10.6	5.7	25.9	LH2_15cm	930	.36		0	2000
					LD2_15cm	280				1000
					C_6%	40				400
					FE_9%	12	3.5	4.7	.04	400
					AU_12%	4.5				100
12.0	18.3	11.9	7.3	22.4	LH2_15cm	180	.078		0	1000
					LD2_15cm	73				500
					C_6%	11				300
					FE_9%	3.2	1.7	.51	.01	200
					AU_12%	1.2				100
15.0	21.0	13.0	8.9	19.9	LH2_15cm	55	.023		0	400
					LD2_15cm	26				300
					C_6%	3.7				200
					FE_9%	1.2	0.9	.10	.002	100

a type of scaling reminiscent of "local duality" in the nucleon persists in the nucleus. To provide new data with which to challenge and constrain the role of QCD in the nucleus, we propose to extract the nuclear structure function F_2^A in a previously unexplored kinematic regime, via high energy electron scattering from nuclei at large x and large Q^2.

2.2 Physics Motivation

With the initial observation by the EMC collaboration [I.1] that the nuclear medium has a significant effect on the nucleon structure function, numerous theoretical studies have attempted to explain the data. From all these analyses it is clear that the presence of other nucleons within $\lesssim 1$ fm can alter the simple perturbative QCD picture of deep inelastic scattering. By probing the nucleons in a nucleus at $x > 1$, a kinematic domain forbidden for the free nucleon, we are directly attacking the nuclear medium effects on the quark structure of the nucleus. Measurements of F_2^A over the full kinematic range are crucial to understanding the role of quark degrees of freedom in the nucleus.

In order to address the physics of inelastic scattering at $x > 1$ we should first consider the behavior of the nucleon structure functions as $x \rightarrow 1$. It was shown by Drell and Yan [II.9] and West [II.10] that the deep inelastic structure functions of the nucleon connect smoothly with the elastic nucleon form factors. In addition, Bloom and Gilman [II.11] discovered that, in the resonance region, the resonance form factors fall with Q^2 at the same rate as the scaling structure functions. They observed that the resonance peaks seen at low Q^2 could be averaged over a finite range in x to yield the high Q^2 deep inelastic structure function. This duality between the scaling structure functions and the elastic and resonance form factors was initially discussed in a simple parton model [II.12]. DeRujula, Georgi, and Politzer [II.13] showed that this local duality was expected from perturbative QCD and should also be valid for the nucleon elastic peak at $(x = 1)$ if the structure functions were analyzed in terms of the Nachtmann variable $\xi = 2x/[1 + (1 + 4M^2x^2/Q^2)^{1/2}]$. This is the correct variable [II.14] in which to study scaling violations at finite Q^2 and accounts for the finite target mass M. In this picture the elastic peak and resonances do not "disappear" into the DIS continuum but instead move to larger ξ, while maintaining a nearly constant strength with respect to the DIS structure functions, which fall rapidly with increasing ξ. There is thus a simple duality between the perturbative aspects of QCD and more complex "higher twist" effects [II.13] which should dominate as $x \rightarrow 1$ at moderate Q^2.

Let us now consider the nuclear structure function for $x > 1$. From a recent analysis [II.7] of SLAC experiment NE3 [II.8] shown in Fig. II.1, we see the structure function per nucleon for Fe as a function of x, for a Q^2 range of 1–4 $(\mathrm{GeV/c})^2$. The increasing

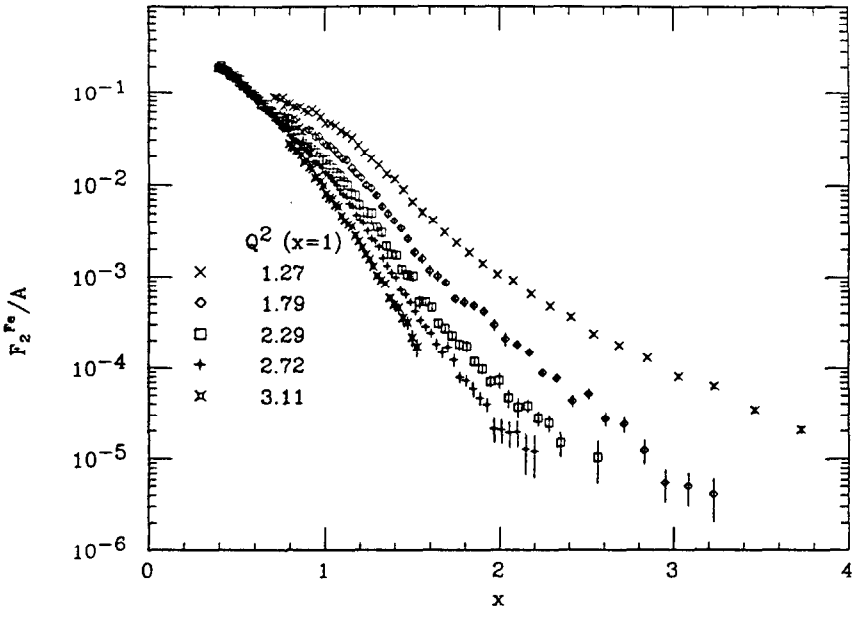

Figure II.1. Measured structure function per nucleon for Fe vs. x from SLAC experiment NE3. The Q^2 value at $x = 1$ is also listed for each kinematics.

separation of the data at large x for different Q^2 can be attributed to the dominance of quasielastic scattering at larger x. Here the Q^2 dependence is governed by the nucleon elastic form factors $G_E(Q^2)$ and $G_M(Q^2)$, which fall rapidly with increasing Q^2. At lower x, deep inelastic scattering (which should have little Q^2 dependence) becomes more important. Thus we observe the expected dominance of Fermi-smeared deep inelastic scattering at medium x and quasielastic scattering at high x.

However, a completely different picture emerges if we consider F_2^A vs. the Nachtmann variable ξ, with the nucleon as the characteristic mass. This is displayed in Fig. II.2 for the **same** data as in Fig. II.1. Here we see that at low ξ the data cluster around a single curve, while at larger ξ they appear to approach this universal curve from below. We emphasize however that this data is for a very limited range of Q^2.

This apparent scaling of the nuclear structure function vs. the Nachtmann variable, suggests a possible link with another kind of scaling observed in nuclei: y-scaling [II.15,16]. Here, in the simplest picture, the electron-nucleus cross section is divided by the elastic nucleon cross section yielding a universal function $-F(y)-$ which is independent of Q^2 and can be related to the light cone momentum distribution of the nucleons in the nucleus [II.6]. The relation between the scaling of $F(y)$ and $F_2^A(\xi)$ is, however, not presently understood. In the simplest relativistic definition y can be related to ξ via $y = M(1 - \xi - \delta)/(1 + \delta)$ where $\delta = M^2\xi^2/Q^2$. For the previous data at $Q^2 < 4$ (GeV/c)^2, there is still a very

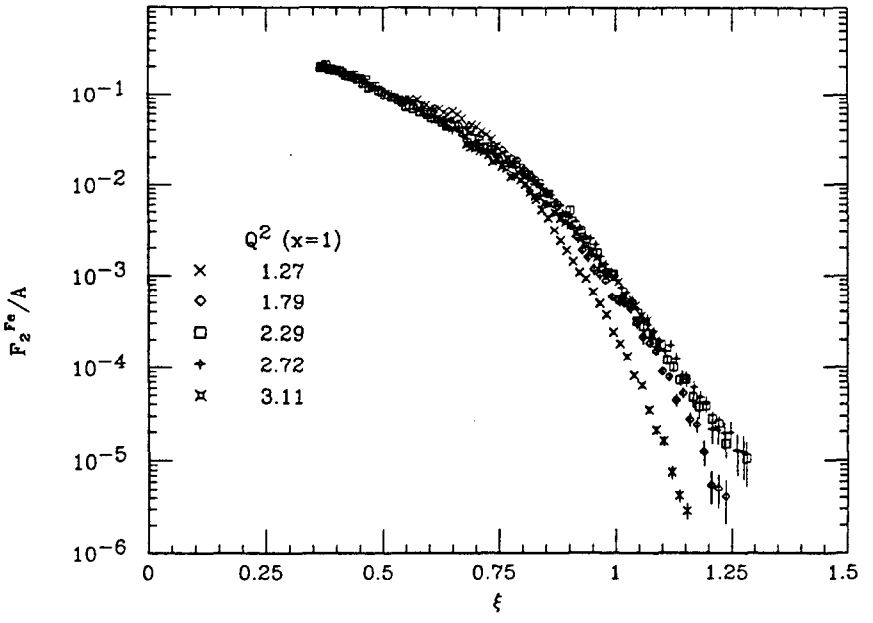

Figure II.2. Measured structure function per nucleon for Fe vs. ξ.

large Q^2 dependence to this expression. But data such as proposed here, by extending the measurements an order of magnitude in Q^2, can seriously explore this connection.

The inclusive data at moderate Q^2 and large values of x also may have a bearing on the question of color transparency discussed in Section I of this proposal. In this kinematic region, the cross section is dominated by quasielastic scattering from individual nucleons including important contributions from the final-state interaction of the struck nucleon. The scattered electron is sensitive to the interaction of the recoil nucleon over a distance of order $1/Q$. If over this region the final-state interaction is significantly reduced due to color transparency, the effect will show up in the inclusive spectrum as well.

This possibility has recently been explored in Benhar *et al.* [II.17], where an extrapolation of previous inclusive data from nuclei [II.18] is compared to a nuclear matter calculation. The calculation is based on a nuclear matter spectral function obtained from the correlated nuclear many body problem, and calculated by accounting for the recoil-nucleon final-state interaction using correlated Glauber theory. The comparison with the extrapolated data suggests that color transparency effects can be important and that a study of the inclusive response at medium Q^2 thus can provide a valuable complement to the investigation of color transparency at large Q^2 via (e,e'p).

The proposed experiment can provide important information on short-range correlations (i.e., high momentum components), non-nucleonic degrees of freedom, and higher twist effects in nuclei. In addition if the $F_2^A(\xi)$ behavior is in fact a scaling phenomena and

persists to higher Q^2 one can hope to extract the large x, scaling limit nuclear structure function from moderate Q^2 inclusive scattering without "interference" from quasielastic scattering.

The use of two spectrometers and several nuclear targets will also allow us to obtain new information on both $R = \sigma_L/\sigma_T$ and nuclear structure function ratios. As discussed below there will be enough overlap in the kinematics of the two spectrometers that a value for R can be extracted with an uncertainty of $\Delta R = \pm(0.1 - 0.2)$ for $x = .5 - 1.0$ and $Q^2 = 10 - 20$ GeV^2. This data can provide important constraints on the structure of the constituents in the transition region between leading-twist deep inelastic scattering from quarks (with $R \to 0$) and possible higher twist contributions, e.g. diquarks (with $R \to \infty$). Because we propose to take data with deuterium as well as carbon and iron targets, we will also be able to construct EMC-type ratios (e.g. F_2^{Fe}/F_2^D). These ratios at $x > 1$ have recently been shown [II.19] to be especially sensitive to high momentum components in the nuclear wavefunctions, with an expected scaling with Q^2 that allows an extraction of the nucleon light-cone momentum distribution in the nucleus.

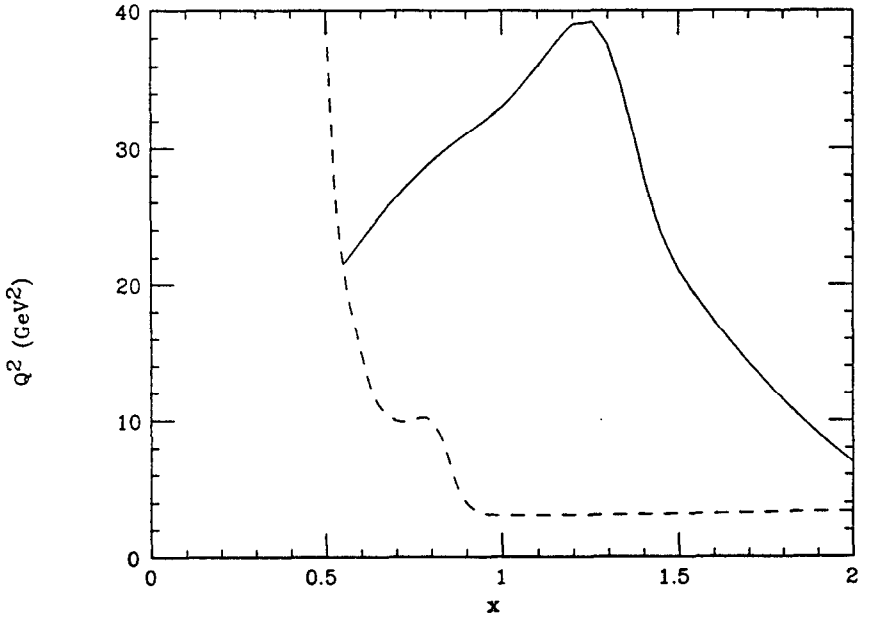

Figure II.3. The kinematic range in x and Q^2 accessible with the proposed experiment are shown. The region below the dashed line has been studied in previous SLAC and CERN experiments. The region between the solid and dashed lines can be studied with the proposed experiment.

The kinematic flexibility of the full SLAC linac with high current and long pulse beam combined with the proposed 16 GeV/c spectrometer and the present 8 GeV/c spectrometer

in End Station A make this experiment possible. The kinematic domain accessible with the proposed experiment is shown in Fig. II.3. Also shown are the region in Q^2 and x where the nuclear structure function has previously been measured. The proposed experiment would thus concentrate on a kinematic region which is largely unexplored.

2.3 Experimental Overview

The experiment utilizes the 16 GeV/c spectrometer discussed in Section III and the 8 GeV/c spectrometer in the large solid angle optics mode, with both detecting scattered electrons simultaneously. In order to extract F_2^A from the measured inclusive cross section a number of corrections and backgrounds must be dealt with.

The measured inclusive spectrum must be corrected for radiative effects in the target and at the scattering vertex. This can be accomplished using a model for the cross section and an iterative "bootstrap" procedure that is very reliable after the first few points have been corrected. Our experience from the analysis of NE3 indicates that the radiative correction procedure is very insensitive to the model used. We estimate that the error in the final cross sections due to radiative corrections will be less than 2%.

In order to extract the structure function, νW_2, from the measured cross section without doing a full Rosenbluth separation (i.e. an angular distribution at fixed Q^2 and ν) a knowledge of $R = \sigma_L/\sigma_T$ is required. We can write the structure function in terms of the measured deep inelastic scattering cross section $\sigma_{Tot} = d^2\sigma/dE'd\Omega$ and R as

$$\nu W_2 = \nu(\sigma_{Tot}/\sigma_{Mott})\frac{1}{1+\beta}$$

where

$$\beta = 2tan^2(\theta/2)\frac{(1+\frac{Q^2}{4M^2x^2})}{(1+R)}.$$

Uncertainties in the value of R can lead to uncertainties in the structure function at large angles as seen from the definition of β above. Contributions to R in the x range of this experiment can result from Fermi-smeared deep inelastic scattering as well as quasielastic nucleon scattering. The data on R for Fe in the deep inelastic range [II.20] indicate that $R_{\rm Fe}^{\rm DIS} < 0.5$ (with little nuclear mass dependence) for $Q^2 = 1$–5 GeV^2 and $x = 0.2$–0.5. A reasonable description of the data is provided by $R_{\rm Fe}^{\rm DIS} = \frac{0.5}{Q^2}$ with Q^2 in (GeV/c)^2 and with little x dependence. For the quasielastic contribution, an impulse approximation estimate yields $R^{QE} \simeq \frac{G_E^2}{\tau G_M^2}$, where $\tau = \frac{Q^2}{4M^2}$, and G_E, G_M are the elastic electric and magnetic form factors. To see the sensitivity of the proposed experiment to uncertainties in R, we assume the above parameterizations of R with an uncertainty range of $\Delta R = \pm 0.25$.

This leads to a worst case uncertainty for the proposed measurement of ± 15% in the determination of the structure function. In order to minimize the uncertainty associated with this correction, we plan to take data with the 8 GeV/c spectrometer at 60° at the lowest three beam energies. This will allow us to extract R at $Q^2 \sim 12 - 20$ (GeV/c)^2 with an uncertainty of $\Delta R = \pm(0.1 - 0.2)$ from $x = 0.5 - 1.0$, and provide us with enough information to minimize uncertainties due to finite values of R.

Parameterizations of previous data indicate that at the largest angle and smallest momentum of this experiment the ratio of π^-/e^- may be as high as $\sim$ 1000. The π rejection factor of $10^4 - 10^5$ from the existing detector package in the 8 GeV/c spectrometer should keep the uncertainty due to π backgrounds to $\sim$ 5%.

The presence of background electrons from charge symmetric processes (e.g. Dalitz pairs and γ conversion) can be checked by reversing the spectrometer momentum and measuring the yield of e^+. Estimates of this background indicate that the subtraction may be as much as 50% at the lowest x and largest angle resulting in an uncertainty of $< 5\%$ in the cross section (the charge symmetry of these processes on nuclei has been checked at the level of a few %).

2.4 Run Plan

The two spectrometers complement each other in their kinematic range. The 16 GeV/c spectrometer is used to access large x up to $Q^2 = 20$ (GeV/c)^2, while the 8 GeV/c can reach smaller x but at higher Q^2 (~ 40 (GeV/c)^2). There will also be some data taken at similar x and Q^2 but different angles in order to gain information on R as discussed above.

In order to estimate counting rates and running times we have attempted to scale the previous data from SLAC experiment NE3. The approximate scaling in ξ discussed above provides a useful guide, so we have taken the highest Q^2 results and assumed no further dependence on Q^2; thus the structure function is assumed to depend only on ξ.

The run plan for the proposed experiment is shown in Table II.1. Counting rates are the main limitation to the kinematic range of the experiment, with a minimum of $\sim$ 0.5 counts/hr at the center of the spectrometer acceptance being the assumed limit. For estimating running times we have assumed 120 pulses per second and 5×10^{11} electrons per pulse from the full linac. The range in x is determined (at low x) by the desire to overlap with existing SLAC data (NE3 and E139) and restricted (at high x) by small counting rates. The running times were calculated for a fixed fractional x bin of $\frac{\Delta x}{x} = 0.05$. The uncertainty is calculated from the number of counts in the central x bin. In order to cover the full range in x, the 8 GeV/c and 16 GeV/c spectrometers' momentum will be stepped

References

[II.1] J. J. Aubert et al., Phys. Lett. **123B**, 275 (1983).
[II.2] A. Bodek, et al., Phys. Rev. Lett. **51**, 534 (1983),
[II.3] R. Arnold, et al., Phys. Rev. Lett. **52**, 727 (1984).
[II.4] J. Vary, Lect. Notes in Phys. **260**, 422 (1986).
[II.5] L. L. Frankfurt and M. I. Strikman, Phys. Rep. **76**, 215 (1981), and L. L. Frankfurt and M. I. Strikman, Phys. Rep. **160**, 235 (1988).
[II.6] Xiangdong Ji and B. W. Filippone, Phys. Rev. **C42**, R2279 (1990).
[II.7] B. W. Filippone, et al., accepted Phys. Rev. **C**
[II.8] D. B. Day *et al.*, Phys. Rev. Lett. **59**, 427 (1987).
[II.9] S. D. Drell and T. M. Yan, Phys. Rev. Lett. **24**, 181 (1970).
[II.10] G. B. West, Phys. Rev. Lett. **24**, 1206 (1970).
[II.11] E. Bloom and F. Gilman, Phys. Rev. **D 4**, 2901 (1971).
[II.12] R. P. Feynman, *Photon Hadron Interactions*, (W. A. Benjamin, Inc. Reading, MA, 1972).
[II.13] A. DeRujula, H. Georgi, and H. D. Politzer, Ann. Phys. **103**, 315 (1977).
[II.14] H. Georgi and H. D. Politzer, Phys. Rev. **D 14**, 1829 (1976).
[II.15] G. B. West, Phys. Rep. **18**, 263 (1975).
[II.16] I. Sick, D. B. Day, and J. S. McCarthy, Phys. Rev. Lett. **45**, 871 (1980).
[II.17] O. Benhar *et al.*, Phys. Rev **C44**, 2328 (1991).
[II.18] D. B. Day *et al.*, Phys. Rev. **C40**, 1011 (1989).
[II.19] L. Frankfurt, M. Strikman, D. Day, and M Sargsyan, (preprint).
[II.20] S. Dasu *et al.*, Phys. Rev. Lett. **60**, 2591 (1988), and Phys. Rev. Lett., **61**, 1061 (1988).

III. Spectrometers

We will run with the 8 GeV/c spectrometer configured in its large acceptance mode. This is attained by running the front quadrupoles Q81 and Q82 with reverse polarities and increasing their field strengths by about a factor of two. The solid angle for the central momentum bin is constant at 3.4 msr up to 4.5 GeV/c. For higher momenta, the solid angle falls off like $1/p^2$ because the first quadrupole is at its maximum at 4.5 GeV/c. The resulting optics preserves the line to point focussing in the horizontal plane and point to point focussing in the vertical plane. During recent E140′ and NE18 running, data were taken with the 8 GeV/c spectrometer tuned in this large acceptance configuration. Elastic and inelastic data were taken at several spectrometer momenta. On-line analysis is in good agreement with Monte Carlo calculations.

The 16 GeV/c spectrometer consists of two bending magnets and three quadrupoles. It will be assembled from magnetic elements from the SLAC 20 GeV/c spectrometer which has been disassembled for the needs of the E142 experiment. The concrete structure required to shield the detectors from room background will be the existing detector hut of the 20 GeV/c spectrometer. The spectrometer will be at a fixed angle of 13.5° with respect to the incident electron beam direction and will point to the ESA target pivot. A schematic of the spectrometer system and the detectors is given in Fig. III.1

The spectrometer system has been designed to provide point-to-point optics in the bend plane (vertical) and parallel-to-point optics in the non-bend plane (horizontal) as can be seen in Figs. III.2 and III.3. The maximum central momentum is 16 GeV/c. The angular dispersion in the non-bend plane is 1.5 cm/mr. The momentum dispersion and the magnification in the bend plane are 2.8 cm/% and 3.3 cm/cm (D/M=0.8).

The expected first-order resolutions are 0.14% for the relative momentum measurement, 0.1 mr for the scattering angle in the horizontal direction and 2.3 mr for the angle in the vertical direction. The spectrometer resolutions have been calculated for the tracking resolutions of the wire chamber system. The momentum acceptance of the spectrometer extends from −10% to +10%. The solid angle for the central momentum bin is 1.0 msr. The average solid angle in the ±10% momentum range is 0.9 msr. The accepted angular ranges are ±27 mr is the bend plane and ±10 mr in the non-bend plane for a target length of 3.5 cm (at 90°) as can be seen in Figs. III.2 and III.3.

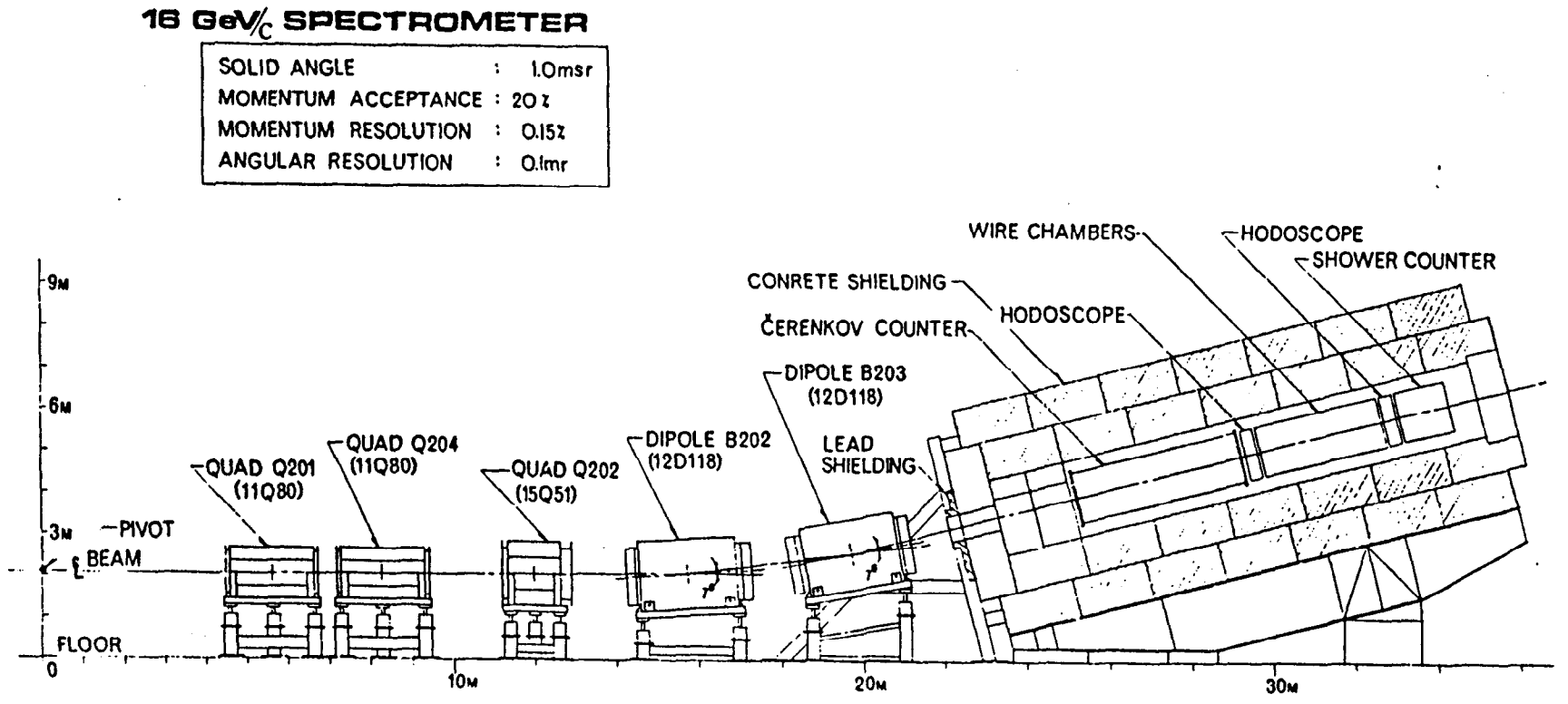

Figure III.1. The proposed 16 GeV/c spectrometer system and the electron detection package. The dipoles 12D118 are the B202 and B203 dipoles from the 20 GeV/c spectrometer. The quadrupoles 11Q80 and 15Q51 are the quadrupoles Q201, Q204 and Q202 from the 20 GeV/c spectrometer. The concrete shielding structure surrounding the detectors is the existing detector hut of the 20 GeV/c spectrometer.

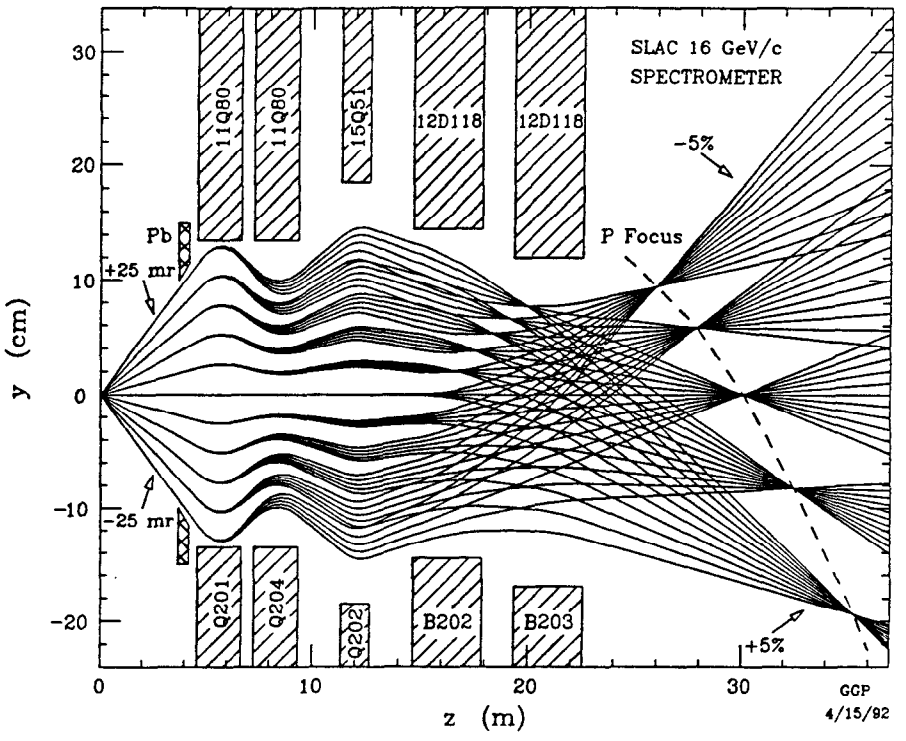

Figure III.2. Bend plan raytrace for rays of different relative momenta originating from the target. All rays are drawn with respect to the central trajectory of the system. Also shown are the magnet pole pieces and lead collimators.

IV. Detectors & Targets

4.1 Detectors

The detectors for the two spectrometers can be assembled using existing components from the 1.6 GeV/c and 8 GeV/c spectrometer detector packages. The desire to have electron identification in both spectrometers leads to the requirement of two 20 radiation length lead glass shower counters with a cross sectional area of 45 x 105 cm^2 for the 16 GeV/c and 40 x 80 cm^2 for the 8 GeV/c. All 14 (10 in use + 4 spare) multi-wire proportional chambers (MWPC) of the 8 GeV/c spectrometer will be used, 8 in the 16 GeV/c and 6 in the 8 GeV/c spectrometer.

The 16 GeV/c spectrometer will be used to detect electrons and be set at a fixed angle of 13.5° throughout the experiment. The 16 GeV/c detector package will consist of a 4 m long gas Cerenkov counter and a lead glass array for π/e rejection, and 8 planes of MWPC for tracking. In addition, we will install the present 1.6 GeV/c scintillator hodoscope for precise timing. The Cerenkov counter will be constructed by adding a 2.5 m

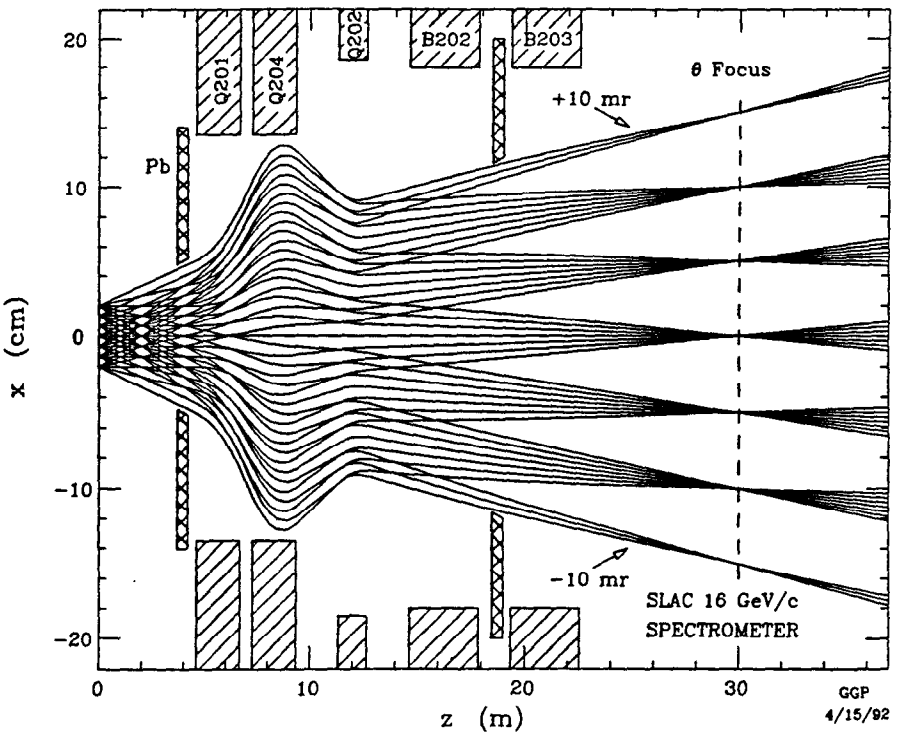

Figure III.3. Non-bend plane raytrace for 0% relative momentum rays originating from different target positions. All rays are drawn with respect to the central trajectory of the system. Also shown are the magnet pole pieces and lead collimators.

cylindrical extension to the existing 1.6 GeV/c Cerenkov counter. It will be filled with CO_2 at a pressure of 0.15 atmospheres, giving a pion threshold of 12.6 GeV/c and an electron efficiency of 98% (4 photo-electrons expected). The lead glass array will be built from 24 out of the 27 SF5 (40 by 14.6 by 14.6 cm) blocks currently used in the 8 GeV/c. Existing electronics modules from the 1.6 GeV/c detector setup and from the Counting House A electronics pool can be used such that no additional acquisition of electronics should be necessary for the 16 GeV/c spectrometer.

The 8 GeV/c detector package will consist of the standard 8 GeV/c Cerenkov counter, 6 of the 10 planes of the MWPC and a lead glass array. The scintillator hodoscope which was rebuilt for experiment NE18 will be used for timing and coarse position measurement. This configuration will work well for hadron as well as for electron detection. For the color transparency experiment, the 8 GeV/c spectrometer will be used to detect recoil protons in coincidence with quasielastically scattered electrons detected in the 16 GeV/c spectrometer. For pion rejection we will run with 1 atmosphere of Freon 12 in the Cerenkov detector with a threshold for pions of 3.0 GeV/c. For the $x > 1$ experiment we will use 0.5

atmospheres of CO_2 in the Cerenkov with a threshold for pions of 7 GeV/c to discriminate between pions and electrons. The lead glass array will be composed of the existing preradiator plane with the addition of 32 F6 (25 by 10 by 10 cm) blocks currently used in the 1.6 GeV/c. The present electronics setup for the 8 GeV/c spectrometer can be used and will not require acquisition of more electronics modules.

In these experiments the random scintillator rates in the two spectrometers are expected to be high. As an example, in the NE18 experiment the singles rate at the first scintillator plane in the 8 GeV/c spectrometer could be as high as 17 per 1.6 μs spill, while the real particle rate was typically $\lesssim$ one per spill. This high rate of random hits did not cause serious problems since the readout time of the MWPCs is only $\approx$ 50 ns. In the proposed experiment we intend to exploit this short readout time after the trigger in both spectrometers.

4.2 Targets

We will require a hydrogen target 15 cm in length, with corresponding dummy target for elastic runs, to measure timing, missing energy, and recoil momentum resolutions and also to set up the quasielastic kinematics. The extended target length is somewhat constrained by the acceptance of the 8 GeV/c spectrometer, but will be easily seen by the 16 GeV/c spectrometer. We will also use a liquid deuterium target of 15 cm length. These are similar to targets used in the recent NE17 experiment and should present no difficulties. We will also require 4%, 6%, and 9% r.l. thick solid targets of ^{12}C, 6%, 9%, and 12% targets of ^{56}Fe, and 9% and 12% targets of ^{197}Au.

V. Request

We request a total of one calendar month to carry out measurements of (e,e'p) at the quasielastic peak in the Q^2 range of 6 to 15 $(GeV/c)^2$ on deuterium, carbon, and iron targets. For the $x > 1$ experiment we request 3 calendar weeks. The request assumes a pulse rate of 120 Hz, a beam current of 5×10^{11} electrons per pulse and an efficiency factor of 0.5. The experiments will require beam energies from 8 to 23.5 GeV. A 16 GeV/c spectrometer will be used to detect quasielastically scattered electrons, fixed at an angle of 13.5 degrees. The 8 GeV/c will be used in the large acceptance optics configuration to detect both protons and electrons over the angular range of 19 to 60 degrees. We will require 15 cm liquid hydrogen and deuterium targets and several thicknesses of carbon, iron and gold. We request an additional one week of low pulse rate for calibration of the new 16 GeV/c spectrometer, and to check out the two detector packages.

VI. The Collaboration

R. Arnold, P. Bosted, S. Rock, Z. Szalata, and J. White
American University

K. Coulter, D. Geesaman, R. Holt, H. Jackson,
S. Kaufman, D. Potterveld, and B. Zeidman
Argonne National Laboratory

J. Arrington, E. Beise, E. Belz, B. Filippone(co-spokesman),
W. Lorenzon(co-spokesman), R. McKeown, and T. O'Neill
California Institute of Technology

K. Aniol, M. Epstein, and D. Margaziotis
California State University, Los Angeles

P. Anthony, K. van Bibber, and F. Dietrich
Lawrence Livermore National Laboratory

R. Ent(co-spokesman), N. Makins, and R. Milner(co-spokesman)
W. Turchinetz
Massachusetts Institute of Technology

J. Napolitano
Rensselaer Polytechnic Institute

G. G. Petratos, R. A. Gearhart
Stanford Linear Accelerator Center

A. Feltham, J. Jourdan, G. Masson, and I. Sick
University of Basel, Switzerland

E. Kinney
University of Colorado

D. Beck
University of Illinois, Urbana-Champaign

J. Chen, D. Day, R. Lourie, J. McCarthy, R. Minehart,
J. Mitchell, O. Rondon-Aramayo
University of Virginia

J. van den Brand, H.J. Bulten, and C. Jones
University of Wisconsin-Madison